

Ag—Cu—Ti 钎料钎焊金刚石的界面微观组织分析

卢金斌^{1,2}, 徐九华²
(1. 中原工学院 材料与化学工程学院, 郑州 450007;
2. 南京航空航天大学 机电学院, 南京 210016)



卢金斌

摘 要: 在真空炉中采用 Ag—Cu—Ti 钎料对金刚石磨粒进行了真空钎焊试验, 实现了金刚石与钢基体的高强度连接。采用 SEM 对金刚石与钎料界面、金刚石表面碳化物形貌进行了观察分析, 采用 EDS 分析了金刚石与钎料界面的成分变化, 采用 Raman 对焊后的金刚石结构进行了分析。结果表明, Ag—Cu—Ti 钎料中的 Ti 元素在界面处发生偏析, 并在金刚石表面生成尺寸小于 1 μm 块状 TiC。金刚石在焊接过程的高温中没有发生石墨化, 最后在界面上形成了金刚石/TiC/钎料/钢基体的梯度结合层。
关键词: 钎焊; 碳化钛; 金刚石
中图分类号: TG401 **文献标识码:** A **文章编号:** 0253-360X(2007)08-029-04

0 序 言

金刚石具有高的硬度、高导热性、低摩擦系数、低热膨胀系数、耐磨性和高强度等优异性能, 但烧结与电镀的金刚石磨料均包埋在涂层中, 在金刚石与涂层间不是化学冶金结合。因此, 开发出能牢固连接金刚石与其它金属的焊接工艺及焊接材料是十分必要的。钎焊金刚石工具因其具有高的连接强度、高的出刃而引起业内专家及厂家的研究和产品开发的极大兴趣, 再配合金刚石的有序排布, 使得这种钎焊金刚石单层工具更具竞争力^[1,2]。根据理论分析及文献报道^[1], 碳化物形成元素如 Ti, Cr, Mo, W 等可实现共价键金刚石晶体与金属键金属的冶金结合, 但冶金结合是通过界面的碳化物来得以实现。因此, 碳化物形貌及金刚石自身是否发生石墨化对连接强度具有极为重要的影响, 从而对金刚石颗粒的把持力和改善这类工具的使用性能具有极其重要的意义。以往采用 Ag—Cu—Ti 钎焊金刚石的研究较多^[3-5], 但尚未对金刚石表面生成的碳化物形貌以及是否发生石墨化进行有关报道。

作者采用 Ag—Cu—Ti 活性钎料作为填充材料, 实现了金刚石与钢基体的高强度连接。在钎焊过程中金刚石中的 C 元素与 Ti 反应形成碳化物, 并借助扫描电镜对金刚石表面生成的 TiC 进行了三维的观

察, 最后对金刚石是否发生石墨化进行了检测与分析。

1 试验材料与方法

基体为 45 钢; 金刚石无镀膜, 40~50 目; Ag—Cu—Ti 钎料, 在 VOQ2—80 型真空炉中进行钎焊试验。具体工艺过程为钎焊前对 45 钢基体、金刚石表面用丙酮清洗, 再浸泡在丙酮中用超声波清洗 5 min, 吹干。将 Ag—Cu—Ti 钎料置于钢体表面, 在钎料上分布金刚石磨粒, 加热至钎焊温度保温适宜时间, 随炉冷却至 120 $^{\circ}\text{C}$ 取出, 接头结构如图 1 所示。

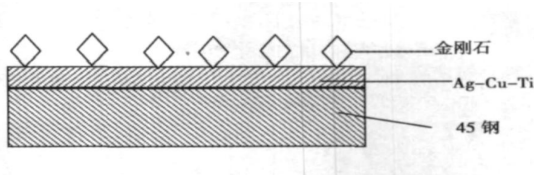


图 1 接头结构示意图

Fig. 1 Joint framework schematic diagram

测试方法: 对焊后的金刚石试样进行深腐蚀, 由于金刚石、碳化物、石墨都是耐腐蚀的, 而金属材料被腐蚀去除, 剩下的就是金刚石与表面生成碳化物。该试样不仅可以用扫描电镜直接观察金刚石表面的三维碳化物形貌, 而且可以用来测试金刚石是否发生石墨化。

收稿日期: 2006-08-23
基金项目: 国家自然科学基金资助项目(50175052); 江苏省自然科学基金资助项目(BK20001049)

测试设备: 用日本电子公司 (JEOL)JSM—6300 型扫描电镜 (SEM) 及美国 KEVEX 公司 X 射线能谱仪 (EDS)。金刚石是否发生石墨化采用的测试设备为法国 JY 公司生产的 IABRAM—HR 激光共焦显微拉曼光谱仪, 可以很准确区别微小区域金刚石与非金刚石, 该光谱仪使用氩离子 514.5 nm 波长的激光, 波数精度为 $\pm 2\text{ cm}^{-1}$, 扫描重复性 $\pm 0.2\text{ cm}^{-1}$ 。光斑直径最小可达 0.01 mm。

2 试验结果与分析

2.1 界面微观组织分析

真空钎焊金刚石后的形貌如图 2 所示, 从图 2 可以看出 Ag—Cu—Ti 钎料对金刚石磨粒表现出很好的浸润性, 金刚石与钎料的加热过程中发生了润湿反应, 钎料沿金刚石侧面达到了一定的高度, 并将金刚石磨粒包裹起来。

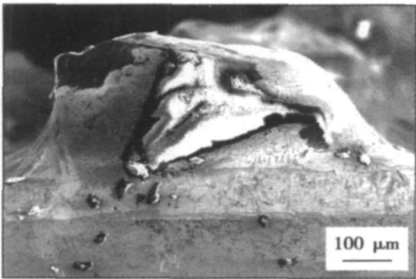


图 2 Ag—Cu—Ti 钎焊金刚石形貌 (SEM)
Fig. 2 Morphologies of brazed diamond

为了分析 Ag—Cu—Ti 钎料中的 Ti 与 C 的相互作用及在接头中的分布情况, 对金刚石和 Ag—Cu—Ti 焊接界面方向取平面, 进行了能谱线扫描成分分析。金刚石与 Ag—Cu—Ti 钎料的焊接界面处 Ag, Cu, Ti, C 各元素的线扫描结果如图 3 所示。可以发现 Ti 元素在金刚石表面有富集。对焊后的金刚石颗

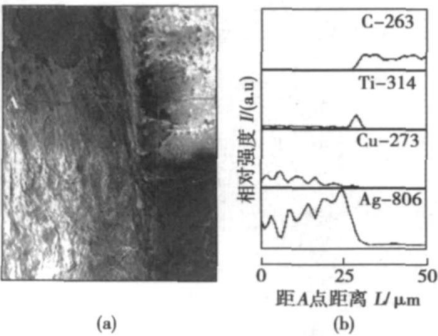


图 3 Ag—Cu—Ti 钎焊金刚石界面元素线分布
Fig. 3 Concentration curves of elements

粒进行长时间深腐蚀进行观察, 其整体形貌如图 4 所示, 从图 4 可以看出金刚石晶体形态完好无损, 棱角清晰, 没有出现裂纹、表面蚀坑等现象。对焊后金刚石表面局部放大观察, 形貌如图 5 所示, 从图 5 可以看到在金刚石表面生成许多豆腐块状的碳化物, 尺寸大多小于 $1\text{ }\mu\text{m}$ 。

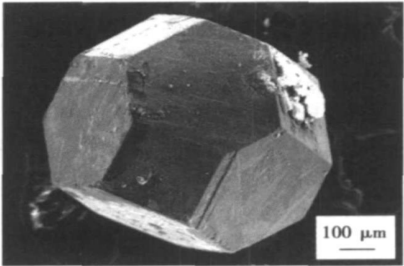


图 4 焊后金刚石形貌
Fig. 4 Morphologies of diamond after brazing

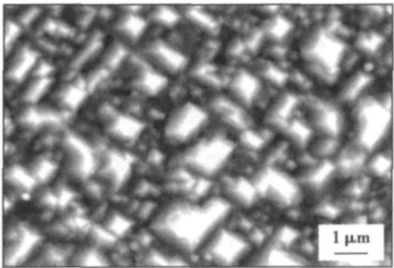


图 5 金刚石表面碳化物形貌
Fig. 5 Morphologies of carbide

文中钎焊结束后在真空炉中自然冷却, 属于低冷却速度近平衡条件, TiC 依靠其生长界面上存在的为数不多的生长台阶以侧向生长方式沿其优先生长方向 $\langle 001 \rangle$ 长大。钎料熔体中 Ti 元素扩散充分, 最终高指数晶面生长速度较快而消失, 低指数晶面因生长速度慢得以保留。金刚石表面 TiC 的生长形态为规则的块状, 并且其分布是有规律的, TiC 晶面几乎全部平行, 这可能是当钎料中的活性 Ti 原子扩散到金刚石表面时, Ti 和 C 的浓度积符合形核条件时在金刚石表面形核时表面能最小, 同时 TiC 生长在单晶的金刚石基体上, 并且 TiC 与金刚石界面肯定有一个最佳的适宜 TiC 生长的方向, 因此 TiC 生长在一个原子排列整齐的表面形成规整且有一定方向性的 TiC。随着反应时间的延长, Ti 原子的不断向界面扩散, TiC 的合成反应不断进行, TiC 晶核不断增多, 并使熔体中的 Ti 原子的含量不断降低, 当其浓度积降至临界浓度积以下时, 合成的 TiC 不

能以晶核的形式稳定存在, 只能向原有的 TiC 晶核上堆积, 使之不断长大, 直到合成的 TiC 与熔融钎料达到平衡为止。TiC 晶体为立方晶系, 晶体空间群 $Fm\bar{3}m(225)$, 属于 NaCl 型晶体结构, 钛和碳都处于面心立方晶格的节点, 由 $a(1/2, 1/2, 1/2)$ 相互取代^[6]。从上面的分析可以知道, 在金刚石表面有块状 TiC 生成, 对金刚石与钎料的界面(图 6)进行仔细观察, 可以看到在金刚石表面有一层黑色的物质存在, 同时可以看到在黑色的物质的外面有一层白色的物质存在, 对其进行能谱测定主要成分为 Ag 元素。那么为什么 Ag 在 TiC 的上面, 必须考虑非均质形核平面错配度和错配能(表 1), 表 1 列出了 Ag, Cu 两种元素与 TiC 间的错配度及界面能^[7]。

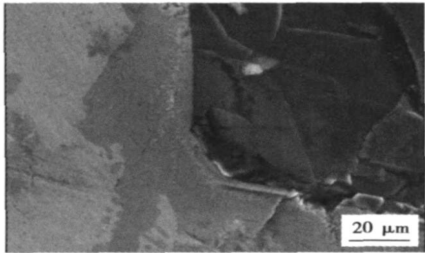


图 6 金刚石与钎料界面形貌图(背散射)

Fig. 6 Morphologies of interface between diamond and brazing filler metal

表 1 Ag—Cu—Ti 钎焊金刚石各化合物间的错配度及界面能
Table 1 Values of planar disregistry and interface energy of Ag—Cu—Ti filler brazing diamond

基体金属	界面	错配度 $\delta(\%)$	TiC 的界面能 $E_{\text{dis}}/(10^{-19}\text{J})$
Cu	Cu(100)—TiC(100)	19.52	1.11
Ag	Ag(100)—TiC(100)	5.728	1.40

从表 1 可以看出, TiC 与 Cu 的平面错配度是 19.52%, 而 TiC 与 Ag 的平面错配度是 5.728%, 这可以解释 Ag 在 TiC 表面的原因。

2.2 激光拉曼光谱测试分析

为了确定钎焊后的金刚石是否发生石墨化, 对焊后的金刚石试样做了激光拉曼光谱分析。

拉曼散射反映材料振动谱特征, 特别对短程结构变化非常敏感。在拉曼谱中, 金刚石和石墨的特征散射峰可以明确无误地区分。同时非晶碳不同的结构构成, 以及相应的 sp^3 , sp^2 键长的变化也会反映在拉曼谱中。当激发光被聚焦到很小的区域(可达微米尺度)时, 获得的微区拉曼信号反应样品特定区域的结

构和成分, 可以被用来区别金刚石和石墨^[8]。

金刚石的拉曼光谱一般可分为两部分: (1) 位于 $1\,332\text{ cm}^{-1}$ 附近典型的金刚石晶体结构的拉曼散射峰, 这个散射峰通常比较锐, 天然金刚石 $1\,332\text{ cm}^{-1}$ 峰的半宽度为 $2\sim3\text{ cm}^{-1}$, 高压法人工合成的金刚石峰的半宽度最小可达 1.7 cm^{-1} ; (2) 位于 $1\,580\text{ cm}^{-1}$ 附近石墨结构成分的拉曼散射峰, 但是多晶石墨还会出现 $1\,358\text{ cm}^{-1}$, $2\,710\text{ cm}^{-1}$ 等散射峰。

图 7 为钎焊后金刚石的拉曼散射特征谱, 从图可以看出金刚石样品 $1\,332\text{ cm}^{-1}$ 特征峰最高, 没有出现任何别的特征峰。因此可以推断采用 Ag—Cu—Ti 对金刚石进行钎焊不会对金刚石造成热损伤。

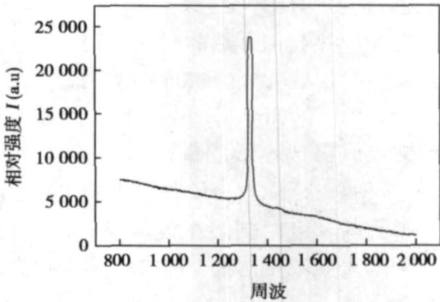


图 7 焊后金刚石的拉曼光谱

Fig. 7 Raman scattering spectra of brazed diamond

Ni—Cr 合金钎焊金刚石表面一般生成的碳化物较多^[2], Ag—Cu—Ti 钎料生成的碳化物较少, 这主要与钎料成分有很大关系, Ni 是促进金刚石石墨化的元素, 并且可以溶解较多的碳, 而 Ag, Cu 对金刚石呈惰性, 因此在液态钎料中含有活性的碳原子较少, 那么只能是活性的 Ti 与金刚石表面碳进行反应, 另外钎焊温度相对较低, 因此金刚石表面的 TiC 含量少, 总的来说, Ag—Cu—Ti 钎料钎焊金刚石表面碳化物大小、分布得比较合理。如果碳化物太多, 不但消耗金刚石本身, 而且脆性的碳化物对连接强度有影响。碳化物太少, 起不到反应润湿的效果, 也对连接强度有影响。

3 结 论

(1) Ag—Cu—Ti 钎料钎焊金刚石实现了金刚石的高强度连接, 其主要是因为是在金刚石表面有 Ti 元素的富集, 并在金刚石表面生成 TiC。

(2) 金刚石与钎料界面生成的 TiC 成规则块状, 其尺寸大多小于 $1\text{ }\mu\text{m}$ 。

(3) 采用 Ag - Cu - Ti 钎料对金刚石进行钎焊不会对金刚石造成热损伤, 金刚石完好无损。

(4) 金刚石表面 TiC 的外侧主要是 Ag, 原因是 Ag 与 TiC 的错配度较小。

参考文献:

[1] 肖 冰, 徐鸿钧, 武志斌 等. Ni - Cr 合金真空单层钎焊金刚石砂轮[J] . 焊接学报 2001, 22(2): 23 - 26.

[2] 卢金斌, 徐九华, 徐鸿钧. Ni - Cr 合金真空钎焊金刚石界面反应的热力学与动力学分析[J] . 焊接学报, 2004 25(1): 21 - 24.

[3] 关砚聪, 陈玉全, 姚德明. Ag - Cu - Ti 钎料钎焊单晶金刚石磨粒的研究[J] . 金刚石与磨料磨具工程, 2005(3): 23 - 25.

[4] 李 丹, 谷 丰, 孙凤莲, 等. CVD 金刚石厚膜钎焊工艺的研究[J] . 应用科技, 2003 6(6): 9 - 10.

[5] 孙凤莲, 冯吉才, 刘会杰, 等. Ag - Cu - Ti 钎料中 Ti 元素在金刚石界面的特征[J] . 中国有色金属学报, 2001, 11(1): 103 - 105.

[6] 金云学, 刘凤伟. 钛合金中 TiC 晶体的生长基元及平衡形态[J] . 稀有金属材料与工程, 2005, 34(10): 1532 - 1536.

[7] Yamazaki T, Suzumura A. Role of the reaction product in the solidification of Ag - Cu - Ti filler for brazing diamond[J] . Journal of Materials Science, 1998(33): 1379 - 1384.

[8] 杨仕娥, 李会军, 边 超. CVD 金刚石膜生长过程的 Raman 分析[J] . 真空与低温, 2002(8): 90 - 92.

作者简介: 卢金斌 男, 1970 年出生, 博士, 讲师。主要从事材料焊接、热处理等领域的科研和教学工作。发表论文 20 余篇。

Email: ljbjohn@163.com

[上接第 28 页]

(2) 在反应热与焦耳热的共同作用下梯度材料的金属陶瓷复合层、Ni₃Al 层、405 不锈钢金属间形成了冶金结合。TiB₂ + Ni/Ni₃Al/405 不锈钢梯度材料 TiB₂ 颗粒被金属镍包裹形成致密的金属陶瓷层, 镍粉与铝粉混合粉末反应生成均匀细小的单相 Ni₃Al。

(3) 得到的梯度材料显微硬度呈梯度变化, 金属陶瓷一侧的表面硬度达到 90 HRA, 具有较高的耐磨损性和热震性。

参考文献:

[1] Robert W, Messler J R Timothyh. Ording fundamentals of the SHS joining process[C] // Materials Research Society Symposium Proceedings, Symposium Held April 12 - 14, San Francisco, California, U. S. A. Joining and Adhesion of Advanced Inorganic Materials 1993, 314: 177 - 182.

[2] Hawk J A, Dogan C P. Self-propagating high-temperature synthesis as a technique to join metals[C] // Materials Research Society Symposium Proceedings, Symposium Held April 12 - 14, San Francisco, California, U. S. A. Joining and Adhesion of Advanced Inorganic Materials 1993, 314: 183 - 194.

[3] Yoshinari Miyamoto, Takashi Nakamoto, Mitsue Koizumi. Ceramic-to-metal welding by a pressurized combustion reaction [J] . Rapid Communications 1986 2(1): 7 - 9.

[4] Ohmi T, Mstura K, Kudoh M. Cemet/ intermetallic joining by centrifugal combustion synthesis[J] . International Journal of Self-Propagating High-Temperature Synthesis, 2004 2(13): 137 - 145.

[5] 张幸红, 韩杰才, 郑永挺, 等. TiC/Ni/TiC 材料的 SHS 合成研究[J] . 材料工程, 1999(6): 33 - 36.

[6] 逢婷婷, 付正义, 张东明. 放电等离子烧结(SPS)技术[J] . 材料导报, 2002 2(16): 31 - 33.

作者简介: 申艳丽, 女, 1979 年出生, 硕士研究生, 助理工程师。主要从事自蔓延高温合成的研究工作。

Email: sy16629@163.com

vanced Materials Processing Technology, Ministry of Education, Beijing 100084, China). p17–20

Abstract: The embedded Real Time Operating System (RTOS) and Micro Controller Operating System-II ($\mu C/OS-II$) are successfully transplanted and applied in the digital-controlled inverter arc welding power supply, which based on the dual Digital Signal Processors. For numerous affairs during welding process after the assignment of multitasks with clear functions, scheduling of multitasks and supervising of multi-states are carried out, and the supervising on the working states of power supply in real time, and the fast and correct judgment and protection action on the faults of power supply, such as the faults of input/output model, the faults of inverter model and the faults of welding assistant equipment etc., are achieved, which guarantees the working reliability and security of welding power supply. Moreover, through the harmony and cooperation of multitasks, the friendly alternation between various working states and users are realized in real time, thus the accuracy of faults identification on power supply system and its maneuverability are improved, and the problems of digital management of real-time states of inverter arc welding power supply and digital comprehensive management of the whole welding machine are solved.

Key words: supervising and management in real time; digital-controlled inverter arc welding power supply; real time operating system; multitasks system

Cutting picker with high chromium Fe-based composite coating prepared by plasma surface metallurgy LIU Junbo (School of Mechanical and Electronic Engineering, Weifang University, Weifang 261061, Shandong, China). p21–24

Abstract: The high chromium Fe-based composite coating was successfully fabricated on the low-carbon low alloy steel by plasma surface metallurgy with the powders which were obtained by heating a mixture powders and sucrose to pyrolyze the sucrose as carbonaceous precursor. The microstructure and microhardness of the coating were studied by scanning electron microscope, X-ray diffraction, energy dispersion spectroscopy and microhardness instrument. Wear and impact test were also analyzed by wear tester and impact tester. The results indicate that the interface between coating and matrix of the composite was metallurgically bonded, and the matching performance of the coating was excellent and each performance advantages were developed. The composite was used to coat cutting picks which simplify the heat-treatment process and reduce the production costs. It indicate that all of the properties surpassed the industry technical standards.

Key words: precursor; reactive plasma surface metallurgy; composite coating; cutting picks

Preparation of $TiB_2 + Ni/Ni_3Al$ stainless steel gradient material via FASHS SHEN Yanli¹, MENG Qingsen¹, Z. A. Munir², XIN Lijun¹, HU Lifang¹ (1. School of Material Science and Engineering, Taiyuan University of Technology, Taiyuan 030024, China; 2. School of Chemical Engineering and Materials Science, University

of California, Davis, USA). p25–28, 32

Abstract $TiB_2 + Ni/Ni_3Al$ stainless steel gradient material was prepared by mechanical alloying and field-activated self-propagating high-temperature synthesis (FASHS). At first, in order to stimulate the combustion reaction, Ni powder and Al powder were mechanical alloying, then $TiB_2 + Ni/Ni_3Al/405$ stainless steel gradient material was prepared by the reaction thermal of self-propagating combustion reaction. The interface, the microstructure and the phase composition of the gradient material were observed by scanning electron microscope and X-ray diffraction, and metallurgical bonding layer was formed in the interfaces of cermet, $Ni_3Al/405$ stainless steel. The mechanical properties, the hardness and the resistance to wear of gradient material were studied by Rockwell hardnessmeter, microhardness tester and grinding abrasion tester, and the results show that cermet surface Rockwell hardness is 90 HRA, and the chemical constitution and the microhardness of material were gradient and the resistance to wear exceed 20Cr case-hardened steel.

Key words: self-propagating high-temperature synthesis; gradient material; cermet; joining

Microstructure of interface between Ag–Cu–Ti brazing filler metal and diamond LU Jinbin^{1,2}, XU Jiu-hua² (1. School of Materials and Chemical Engineering, Zhongyuan University of Technology, Zhengzhou 450007, China; 2. Nanjing University of Aeronautics and Astronautics, Nanjing 210016, China). p29–32

Abstract The high-strength bonding between steel matrix and diamond grit was obtained by using Ag–Cu–Ti brazing filler metal in vacuum furnace. The microstructure on the interface between diamond and the filler metal and carbide which was formed on the diamond surface was observed with scanning electron microscope, and the change of components in it was analyzed with energy dispersion spectroscopy and the structure of the diamond was analyzed with Raman. Results showed that Ti in Ag–Cu–Ti separated out at the interface to form lump-like TiC carbide on the surface of diamond, which was less than 1 μm in size. Meanwhile, the diamond wasn't graphitized in the high temperature. As a result, the serial of diamond-TiC-filler metal-steel matrix was formed between the interface of the diamond and the filler metal.

Key words: brazing; TiC; diamond

Effect of Ag–Al–Ga addition on wettability of Sn–9Zn lead-free solder WANG Hui, XUE Songhai, CHEN Wenxue, WANG Jianxin (College of Materials Science and Technology, Nanjing University of Aeronautics and Astronautics, Nanjing 210016, China). p33–36, 44

Abstract Wettability of Sn–9Zn–X (Ag, Al, Ga) lead-free solder, with non-cleaning flux and $ZnCl_2-NH_4Cl$ flux, was appraised by means of wetting balance method in air and N_2 atmospheres; the effect of different additive amount of Ag, Al, Ga on the wettability of Sn–9Zn–X solders was studied. The results indicate that the optimum additive amount of Ag, Al, Ga in Sn–9Zn solder is 0.3, 0.005–0.02 and 0.5 mass percent, respectively. The wet-